

QUASICRYSTALS: PROJECTIONS OF 5-D LATTICE INTO 2 AND 3 DIMENSIONS

HELEN AU-YANG AND JACQUES H. H. PERK

*Department of Physics,
Oklahoma State University,
Stillwater, OK 74078-3072, USA
E-mail: perk@okstate.edu*

We show that generalized Penrose tilings can be obtained by the projection of a cut plane of a 5-dimensional lattice into two dimensions, while 3-d quasiperiodic lattices with overlapping unit cells are its projections into 3d. The frequencies of all possible vertex types in the generalized Penrose tilings, and the frequencies of all possible types of overlapping 3-d unit cells are also given here. The generalized Penrose tilings are found to be nonconvertable to kite and dart patterns, nor can they be described by the overlapping decagons of Gummelt.

1. Introduction

Quasicrystals, though originally introduced as a mathematical curiosity, have become an object of intense study by physicists and mathematicians following the startling discovery in 1984 of five- or ten-fold symmetry in diffraction patterns off certain alloys.¹ Quasicrystals have been studied most often by filling the space aperiodically with nonoverlapping tiles, such as in Penrose tilings.^{2,3,4} However, in the mid 1990s, Gummelt⁵ proposed a new description of the regular Penrose tiling in terms of the overlapping of decorated decagons. Further research^{6,7,8,9} has shown that this may be a more sensible way to understand quasicrystalline materials—made of overlapping unit cells sharing atoms of nearby neighbors.⁷

We shall use de Bruijn's multigrid method to produce a new example of 3-dimensional overlapping unit cells.¹⁰ Moreover, we shall use the pentagrid method to obtain generalized Penrose tilings, which cannot be converted to kite and dart patterns, nor do they satisfy the inflation and deflation rules. Therefore, since Conway's cartwheels, which are in fact the overlapping decagons of Gummelt, are constructed from kite and dart patterns,³ they cannot be used to describe the generalized Penrose tilings.

2. Grids and the ‘Cut and Projection Method’

It is well-known that a Penrose tiling can be obtained by the projection of a particularly ‘cut’ slice of the 5-d euclidian lattice onto a 2-d plane \mathcal{D} ,^{4,11,12} and that its diffraction pattern,^{13,14,15} therefore, has five- or ten-fold symmetry. It is also known that not all lattice points \mathbf{k} in \mathbb{Z}^5 can be mapped onto vertices of a Penrose tiling; only those points in a particular ‘cut’ slice whose projections into the 3-dimensional orthogonal space \mathcal{W} are inside the window of acceptance,^{11,16} contribute. The window has been shown¹¹ to be the projection of the 5-d unit cell $\text{Cu}(5)$ with 2^5 vertices into this 3-d space \mathcal{W} .

If \mathbf{d}_j are the generators of the plane \mathcal{D} and \mathbf{w}_j are the generators of its orthogonal space \mathcal{W} , then the projection operators are the matrices

$$\mathbf{D}^T = (\mathbf{d}_0, \dots, \mathbf{d}_4), \quad \mathbf{W}^T = (\mathbf{w}_0, \dots, \mathbf{w}_4) \quad (1)$$

satisfying $\mathbf{D}^T \mathbf{W} = \mathbf{W}^T \mathbf{D} = 0$, where the superscript T denotes matrix transposition. More specifically, we choose

$$\mathbf{d}_j^T = (\cos j\theta, \sin j\theta), \quad \mathbf{w}_j^T = (\cos 2j\theta, \sin 2j\theta, 1) = (\mathbf{d}_{2j}^T, 1), \quad (2)$$

where $j = 0, \dots, 4$ and $\theta = 2\pi/5$. Using notations and ideas introduced by de Bruijn,⁴ we consider the 2-d or 3-d pentagrid consisting of five grids of either equidistant lines given by

$$x \cos j\theta + y \sin j\theta + \gamma_j = \mathbf{d}_j^T \mathbf{r} + \gamma_j = k_j, \quad \mathbf{r}^T = (x, y), \quad (3)$$

or equidistant planes defined by

$$x \cos 2j\theta + y \sin 2j\theta + z + \gamma_j = \mathbf{w}_j^T \mathbf{R} + \gamma_j = k_j, \quad \mathbf{R}^T = (x, y, z), \quad (4)$$

for $j = 0, \dots, 4$, and with the five $k_j \in \mathbb{Z}$. In (3) and (4), the γ_j are real numbers which shift the grids from the origin. We denote their sum by

$$\gamma_0 + \gamma_1 + \gamma_2 + \gamma_3 + \gamma_4 = c, \quad 0 \leq c < 1. \quad (5)$$

Without loss of generality, we may restrict c to $0 \leq c < 1$, as we can see from (3) that $c \rightarrow c - n$ if we let $k_0 \rightarrow k_0 + n$. Obviously, such a relabeling cannot change the 2-d or 3-d quasiperiodic patterns.

It has been shown by de Bruijn⁴ that the Penrose tiling associated with a 2-d pentagrid has simple matching rules only for $c = 0$. In other words, for $0 < c < 1$ the corresponding generalized Penrose tilings do not satisfy simple matching rules, and have different sets of vertices for different intervals of c .¹⁷ Nevertheless, the diffraction patterns are believed to be the same for all values of c .^{18,19}

Let the integer k_j be assigned to all points sandwiched between the grid lines or planes defined by $k_j - 1$ and k_j . This k_j can be found by

$$K_j(\mathbf{r}) = \lceil \mathbf{d}_j^T \mathbf{r} + \gamma_j \rceil, \quad \forall \mathbf{r} \in \mathbb{R}^2 \quad (6)$$

$$\tilde{K}_j(\mathbf{R}) = \lceil \mathbf{w}_j^T \mathbf{R} + \gamma_j \rceil, \quad \forall \mathbf{R} \in \mathbb{R}^3 \quad (7)$$

for $j = 0, \dots, 4$, (and $\lceil x \rceil$ is the smallest integer greater than or equal to x). A mesh in \mathbb{R}^2 is an interior area, enclosed by grid lines, containing points with the same five integers $K_j(\mathbf{r})$, while a mesh in \mathbb{R}^3 is now an interior volume, enclosed by grid planes, containing points with the same five integers $\tilde{K}_j(\mathbf{R})$. One then maps each mesh in \mathbb{R}^2 to a vertex in \mathcal{D} by

$$\mathbf{f}(\mathbf{r}) = \sum_{j=0}^4 K_j(\mathbf{r}) \mathbf{d}_j = \mathbf{D}^T \mathbf{K}(\mathbf{r}), \quad \mathbf{K}^T(\mathbf{r}) = (K_0(\mathbf{r}), \dots, K_4(\mathbf{r})), \quad (8)$$

and each mesh in \mathbb{R}^3 to a vertex in \mathcal{W} by

$$\mathbf{g}(\mathbf{R}) = \sum_{j=0}^4 \tilde{K}_j(\mathbf{R}) \mathbf{w}_j = \mathbf{W}^T \tilde{\mathbf{K}}(\mathbf{R}), \quad \tilde{\mathbf{K}}^T(\mathbf{R}) = (\tilde{K}_0(\mathbf{R}), \dots, \tilde{K}_4(\mathbf{R})). \quad (9)$$

The resulting sets of vertices $\mathcal{I} = \{\mathbf{f}(\mathbf{r}) | \mathbf{r} \in \mathbb{R}^2\}$ and $\mathcal{L} = \{\mathbf{g}(\mathbf{R}) | \mathbf{R} \in \mathbb{R}^3\}$ are, respectively, the two- and three-dimensional quasiperiodic lattices.

3. Window of Acceptance

Given a point $\mathbf{k}^T = (k_0, \dots, k_4)$ in the five-dimensional lattice,^a one may ask whether there is a mesh in the pentagrid (or the 3-d multigrad) such that $K_j(\mathbf{r}) = k_j$ (or $\tilde{K}_j(\mathbf{R}) = k_j$) for $j = 0, \dots, 4$. As seen from (6) (or (7)), this is equivalent to asking whether it is possible to find points \mathbf{r} in \mathbb{R}^2 (or \mathbf{R} in \mathbb{R}^3), and points $\boldsymbol{\lambda}^T = (\lambda_0, \dots, \lambda_4)$ with $0 \leq \lambda_j < 1$, such that

$$\mathbf{D}\mathbf{r} + \boldsymbol{\gamma} + \boldsymbol{\lambda} = \mathbf{k}, \quad (\mathbf{W}\mathbf{R} + \boldsymbol{\gamma} + \boldsymbol{\lambda} = \mathbf{k}), \quad (10)$$

where $\boldsymbol{\gamma}^T = (\gamma_0, \dots, \gamma_4)$ and where $\boldsymbol{\lambda}$ lies inside the 5-d unit cube $\text{Cu}(5)$. Whenever (10) holds, the point \mathbf{k} in \mathbb{Z}^5 is said to satisfy the mesh condition. Since $\mathbf{W}^T \mathbf{D} = \mathbf{D}^T \mathbf{W} = 0$, the above equations become

$$\mathbf{W}^T [\mathbf{k} - \boldsymbol{\gamma}] = \mathbf{W}^T \boldsymbol{\lambda}, \quad (11)$$

$$\mathbf{D}^T [\mathbf{k} - \boldsymbol{\gamma}] = \mathbf{D}^T \boldsymbol{\lambda}, \quad (12)$$

^aFor a formulation for more general cases, see Ref. 11.

such that $\mathbf{D}^T \mathbf{k} \in \mathcal{I}$ if (11) holds, or $\mathbf{W}^T \mathbf{k} \in \mathcal{L}$ if (12) holds. Thus, $\mathbf{W}^T \boldsymbol{\lambda}$ is the window of acceptance for projections into 2d and $\mathbf{D}^T \boldsymbol{\lambda}$ for 3d. They are respectively the interiors of the convex hulls of the points $\mathbf{W}^T \mathbf{n}_i$ and $\mathbf{D}^T \mathbf{n}_i$, where the \mathbf{n}_i are the 2^5 vertices of the 5-d unit cube Cu(5).

We choose the 32 \mathbf{n}_i 's as follows

$$\begin{aligned} \mathbf{n}_0^T &= (0, 0, 0, 0, 0), \mathbf{n}_1^T = (1, 0, 0, 0, 0), \mathbf{n}_2^T = (0, 0, 0, 1, 0), \mathbf{n}_3^T = (0, 1, 0, 0, 0), \\ \mathbf{n}_4^T &= (0, 0, 0, 0, 1), \mathbf{n}_5^T = (0, 0, 1, 0, 0), \mathbf{n}_6^T = (1, 0, 0, 1, 0), \mathbf{n}_7^T = (0, 1, 0, 1, 0), \\ \mathbf{n}_8^T &= (0, 1, 0, 0, 1), \mathbf{n}_9^T = (0, 0, 1, 0, 1), \mathbf{n}_{10}^T = (1, 0, 1, 0, 0), \mathbf{n}_{11}^T = (1, 1, 0, 0, 0), \\ \mathbf{n}_{12}^T &= (0, 0, 0, 1, 1), \mathbf{n}_{13}^T = (0, 1, 1, 0, 0), \mathbf{n}_{14}^T = (1, 0, 0, 0, 1), \mathbf{n}_{15}^T = (0, 0, 1, 1, 0), \\ \mathbf{n}_{16}^T &= (1, 1, 0, 0, 1), \mathbf{n}_{17}^T = (0, 0, 1, 1, 1), \mathbf{n}_{18}^T = (1, 1, 1, 0, 0), \mathbf{n}_{19}^T = (1, 0, 0, 1, 1), \\ \mathbf{n}_{20}^T &= (0, 1, 1, 1, 0), \mathbf{n}_{21}^T = (1, 1, 0, 1, 0), \mathbf{n}_{22}^T = (0, 1, 0, 1, 1), \mathbf{n}_{23}^T = (0, 1, 1, 0, 1), \\ \mathbf{n}_{24}^T &= (1, 0, 1, 0, 1), \mathbf{n}_{25}^T = (1, 0, 1, 1, 0), \mathbf{n}_{26}^T = (1, 1, 0, 1, 1), \mathbf{n}_{27}^T = (0, 1, 1, 1, 1), \\ \mathbf{n}_{28}^T &= (1, 1, 1, 0, 1), \mathbf{n}_{29}^T = (1, 0, 1, 1, 1), \mathbf{n}_{30}^T = (1, 1, 1, 1, 0), \mathbf{n}_{31}^T = (1, 1, 1, 1, 1). \end{aligned} \quad (13)$$

The projection of these 32 points into \mathcal{W} is a polytope \mathcal{P} having 20 faces and 40 edges connecting the 22 vertices, as is shown in Fig. 1. We let $\mathbf{P}_i = \mathbf{W}^T \mathbf{n}_i$ for $i = 0, \dots, 31$. The bottom is $\mathbf{P}_0 = (0, 0, 0)$ and top is $\mathbf{P}_{31} = (0, 0, 5)$; they are called the tips of the polytope. The remaining twenty vertices of \mathcal{P} are

$$\begin{aligned} \mathbf{P}_{j+1} &= (\mathbf{d}_j, 1), \quad \mathbf{P}_{j+6} = (\mathbf{d}_j + \mathbf{d}_{j+1}, 2), \\ \mathbf{P}_{j+21} &= (-\mathbf{d}_{j-2} - \mathbf{d}_{j-1}, 3), \quad \mathbf{P}_{j+26} = (-\mathbf{d}_{j-1}, 4), \end{aligned} \quad (14)$$

for $j = 0, \dots, 4$. The other 10 points $\mathbf{P}_{11}, \dots, \mathbf{P}_{20}$ are in the interior of the polytope and are given by

$$\mathbf{P}_{11+j} = (\mathbf{d}_j + \mathbf{d}_{j+2}, 2), \quad \mathbf{P}_{16+j} = (-\mathbf{d}_{j+1} - \mathbf{d}_{j-1}, 3), \quad (15)$$

again for $j = 0, \dots, 4$.

The orthogonal projection of the 32 points \mathbf{n}_i into \mathcal{D} is a decagon \mathcal{Q} with 10 edges connecting the 10 vertices. Let $\mathbf{Q}_i = \mathbf{D}^T \mathbf{n}_i$, for $i = 0, \dots, 31$. Then the vertices of the decagon are

$$\mathbf{Q}_{11+j} = -p\mathbf{d}_{3-2j}, \quad \mathbf{Q}_{16+j} = p\mathbf{d}_{5-2j}, \quad (16)$$

with $j = 0, \dots, 4$, and $p = (\sqrt{5} + 1)/2$ is the golden ratio. The remaining 22 points $\mathbf{Q}_0, \dots, \mathbf{Q}_{10}, \mathbf{Q}_{21}, \dots, \mathbf{Q}_{31}$ are in the interior; they are given by

$$\begin{aligned} \mathbf{Q}_0 &= \mathbf{Q}_{31} = 0, \quad \mathbf{Q}_{j+1} = \mathbf{d}_{5-2j}, \quad \mathbf{Q}_{26+j} = -\mathbf{d}_{2-2j}, \\ \mathbf{Q}_{j+6} &= p^{-1}\mathbf{d}_{4-2j}, \quad \mathbf{Q}_{21+j} = -p^{-1}\mathbf{d}_{3-2j}. \end{aligned} \quad (17)$$

The decagons are shown in Fig. 2. Thus if orthogonal projection $\mathbf{D}^T(\mathbf{k} - \boldsymbol{\gamma})$ is in \mathcal{Q} , then its projection $\mathbf{W}^T \mathbf{k}$ is in \mathcal{L} .

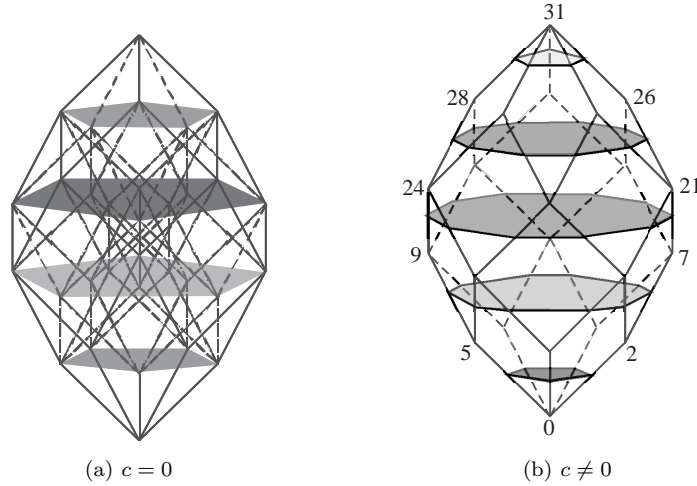


Figure 1. The projection of the 5-dimensional unit cube into the orthogonal 3-space \mathcal{W} . The polytopes with 22 vertices are tilted 10 degree with respect to the vertical, so that the intersections V_I with the planes $z = I - c$ can be seen. In (a), for $c = 0$, we show the projection of the 32 points, 10 of which are in the interior, and the V_I are all pentagons. In (b), for $c \neq 0$, the V_I are pentagons for $I = 1, 5$, and decagons for $I = 2, 3, 4$.

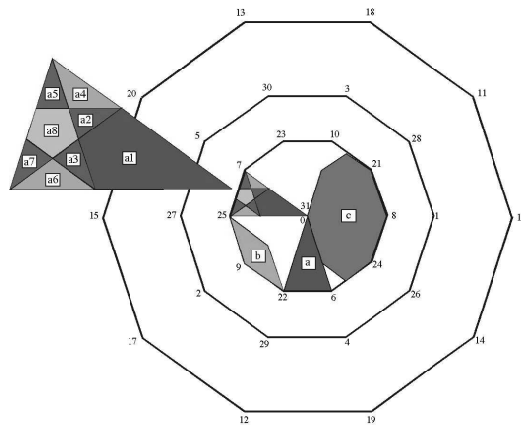


Figure 2. The projection of the 5-d unit cube $Cu(5)$ into the orthogonal 2-d space \mathbf{D} . The window is a decagon Q whose vertices are given by (16). Those n_i which are mapped to interior points (vertices) of \mathcal{P} in Fig. 1, are mapped into the boundary vertices of Q .

4. Generalized Penrose Tilings

Using (1) and (2), we may rewrite the three components of (11) as

$$\sum_{j=0}^4 (k_j - \gamma_j) = I - c = \sum_{j=0}^4 \lambda_j, \quad \sum_{j=0}^4 (k_j - \gamma_j) \mathbf{d}_{2j} = \sum_{j=0}^4 \lambda_j \mathbf{d}_{2j}, \quad (18)$$

where $I \equiv \sum k_j$ is the index of \mathbf{k} , an integer in the interval $[1, 5]$ for $0 < c < 1$. ($I = 5$ does not occur for $c = 0$.) Eq. (18) defines the window V_I for accepting \mathbf{k} with index I . This window V_I is the intersection of the polytope \mathcal{P} with the plane at the height $I - c$ shown in Fig. 1.

For \mathbf{k} in window V_I , we examine the condition for its neighbor \mathbf{k}' , (with $\mathbf{k}' = \mathbf{k} \pm \mathbf{n}_j, j = 1, \dots, 5$), to be in window $V_{I \pm 1}$. Whenever this condition is satisfied, then $D^T \mathbf{k}$ and $D^T \mathbf{k}'$ are both vertices of the generalized Penrose tiling. Furthermore there is a ‘positive’ (‘negative’) edge incident from the image of \mathbf{k} in the direction of \mathbf{d}_{3j} ($-\mathbf{d}_{3j}$) to the image of \mathbf{k}' . This way we can determine all the vertex types of the generalized Penrose tiling for a given c . Denoting all vertices with index I having n ‘positive’ edges and n' ‘negative’ edges by $[n, n']_I$, we find that for $\mathbf{k} \in V_1$ there are only three kinds of vertex types $[5, 0]_1$, $[4, 0]_1$, and $[3, 0]_1$, and for $\mathbf{k} \in V_5$ there are also only three kinds of vertex types $[0, 5]_5$, $[0, 4]_5$, and $[0, 3]_5$, shown in Fig. 3a.

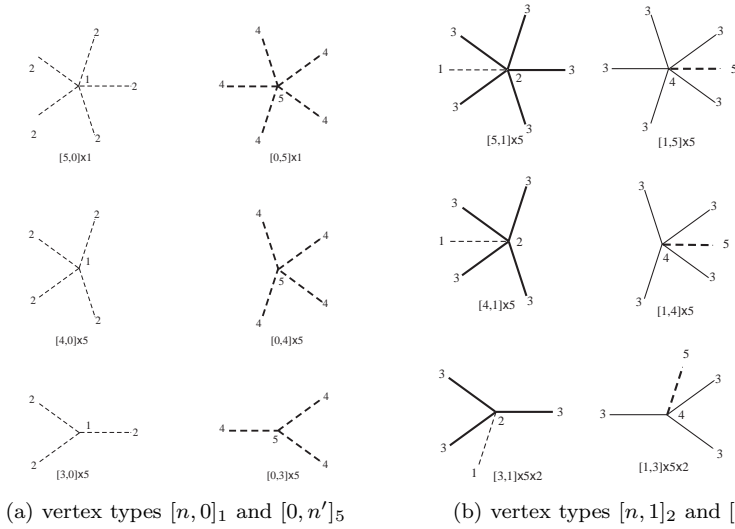


Figure 3. (a) Edges connecting two sites with indices 1 and 2 are represented by thin dashed lines, while edges connecting sites with indices 5 and 4 are represented by thick dashed lines. (b) A few examples of vertex types $[n, 1]_2$ and $[n, 1]_4$ are given here. Edges connecting sites with indices 2 and 3 are denoted by thick lines, and edges connecting sites with indices 3 and 4 by thin lines. We use $[n, n'] \times 5$ to indicate the 5-fold multiplicity under 72° rotations allowed for the vertex, and $[n, n'] \times 5 \times 2$ to indicate the additional reflection symmetry when it is present.

If the probability of finding a vertex of type $[n, n']_I$ is denoted by

$A_I(n, n')/5p$, then

$$\begin{aligned} A_1[5, 0] &= \frac{1}{2}(p^{-1}+p)p^{-3}(1-c)^2, \\ A_1[4, 0] &= \frac{5}{2}p^{-4}(1-c)^2, \quad A_1[3, 0] = \frac{5}{2}p^{-3}(1-c)^2, \end{aligned} \quad (19)$$

while $A_5[0, n]$ is given by replacing $1-c$ in $A_1[n, 0]$ by c .

There are nine different vertex types for $I = 2, 4$, see Fig. 3b for some examples of each type. Their frequencies are

$$\begin{aligned} A_2[5, 0] &= \frac{1}{2}(p^{-1}+p)[\theta(p^{-2}-c)(p^{-3}+c)^2 + \theta(c-p^{-2})p^{-4}(2-c)^2], \\ A_2[5, 1] &= \theta(p^{-2}-c)\frac{5}{2}(p^{-5}+c)p(p^{-2}-c), \\ A_2[5, 2] &= \theta(p^{-2}-c)\frac{5}{2}p^{-1}(p^{-2}-c)^2, \\ A_2[4, 0] &= \theta(c-p^{-2})\frac{5}{2}(c-p^{-2})[p^{-1}(1-c) + p^{-3}(2-c)], \\ A_2[4, 1] &= \theta(p^{-2}-c)\frac{5}{2}p^{-1}c^2 + \theta(c-p^{-2})\frac{5}{2}p^{-3}(1-c)^2, \\ A_2[3, 2] &= \theta(p^{-2}-c)\frac{5}{2}p^2(p^{-2}-c)^2, \\ A_2[3, 1] &= 5p^{-2}(1-c)^2 - \theta(p^{-2}-c)5p^2(p^{-2}-c)^2, \\ A_2[3, 0] &= \frac{5}{2}c^2 - \theta(c-p^{-2})5(c-p^{-2})^2, \\ A_2[2, 1] &= \frac{5}{2}p^{-1}(1-c)^2, \end{aligned} \quad (20)$$

where $\theta(x)$ is the Heaviside function, *i.e.*, $\theta(x) = 1$ for $x \geq 0$, and zero otherwise. We find that the open interval $0 < c < 1$ is split into two intervals $0 < c < p^{-2}$ and $p^{-2} < c < 1$. Inside the former interval, $A_2(4, 0) = 0$, and only eight kinds of vertices are allowed; inside the latter, $A_2(5, 2) = A_2(5, 1) = A_2(3, 1) = 0$, allowing only six vertex types. At the boundary $c = 0$ or $c = p^{-2}$, there are only five allowed vertex types. We find that $A_4[n, n']$ can be obtained from $A_2[n', n]$ by $c \rightarrow 1-c$. Now for c in the interval $0 < c < p^{-1}$ there are six nonvanishing vertex types, while inside the interval $p^{-1} < c < 1$, there are eight nonvanishing vertex types.

There are many vertex types $[n, n']_3$. Twelve out of twenty of their frequency functions $A_3[n, n']$ are given as

$$\begin{aligned} A_3[0, 5] &= \theta(p^{-3}-c)\frac{1}{2}(p^{-1}+p)(p^{-3}-c)^2, \\ A_3[1, 5] &= \theta(p^{-3}-c)\frac{5}{2}(p^{-3}-c)^2, \\ A_3[2, 5] &= \theta(p^{-2}-c)\frac{5}{2}p^2(p^{-2}-c)^2 - \theta(p^{-3}-c)5p^2(p^{-3}-c)^2, \\ A_3[3, 5] &= \theta(2p^{-3}-c)[\frac{5}{2}c^2 - \theta(c-p^{-3})5p^2(c-p^{-3})^2 \\ &\quad + \theta(c-p^{-2})5p^3(c-p^{-2})^2], \\ A_3[4, 5] &= \theta(c-p^{-3})[\theta(p^{-2}+p^{-4}-c)\frac{5}{2}p^3(p^{-2}+p^{-4}-c)^2 \\ &\quad - \theta(2p^{-3}-c)5p^3(2p^{-3}-c)^2 + \theta(p^{-2}-c)5p^2(p^{-2}-c)^2], \\ A_3[5, 5] &= \theta(c-p^{-3})[\theta(2p^{-2}-c)\frac{1}{2}(p+p^{-1})(2p^{-2}-c)^2 \\ &\quad - \theta(p^{-2}+p^{-4}-c)\frac{5}{2}p^3(p^{-2}+p^{-4}-c)^2 + \theta(2p^{-3}-c)\frac{5}{2}p^3(2p^{-3}-c)^2], \\ A_3[3, 4] &= \theta(p^{-1}-c)[\frac{5}{2}p^{-3}c^2 \\ &\quad - \theta(c-p^{-2})5p(c-p^{-2})^2 + \theta(c-2p^{-3})\frac{5}{2}p^3(c-2p^{-3})^2], \end{aligned}$$

$$\begin{aligned}
A_3[4, 4] &= \theta(p^{-1}-c)[\theta(c-p^{-2})5(c-p^{-2})^2 - \theta(c-2p^{-3})5p^3(c-2p^{-3})^2 \\
&\quad + \theta(c-p^{-2}-p^{-4})5p^3(c-p^{-2}-p^{-4})^2], \\
A_3[3, 3] &= 5p^{-4}(1-c)^2 - \theta(p^{-1}-c)5p^{-1}(p^{-1}-c)^2 + \theta(p^{-2}-c)5p^{-1}(p^{-2}-c)^2, \\
A_3[2, 3] &= 5p^{-3}(1-c)^2 - \theta(p^{-2}-c)\frac{5}{2}p^{-1}(p^{-2}-c)^2, \\
A_3[2, 2] &= 10p^{-1}c(1-c), \quad A_3[1, 2] = \frac{5}{2}p^{-1}(1-c)^2. \quad (21)
\end{aligned}$$

The remaining eight $A_3[n', n]$ can be obtained from $A_3[n, n']$ by letting $c \rightarrow 1 - c$. They are continuous functions of c .

We plot in Fig. 4 generalized Penrose tilings for $c = p^{-2} = 0.3819660098$ and $c = 0.5$. We find that the number of vertices of index 1 increases, and of index 5 decreases, as c increases.

5. Overlapping polytope

Consider now the projection of \mathbb{Z}^5 into the 3-d space \mathcal{W} . It is easy to find the conditions for both \mathbf{k} and its neighbors $\mathbf{k} + \mathbf{n}_j$, for $j = 1 \cdots 5$, to satisfy their mesh conditions, so that they are vertices of quasiperiodic lattice \mathcal{L} .

We find that every point inside the innermost decagon $\hat{\mathcal{Q}}$ in Fig. 2 corresponds to a point in \mathcal{L} that is connected with its 10 neighbors, and is in fact a tip of a polytope. This innermost decagon $\hat{\mathcal{Q}}$ is further divided into 10 triangles. Each point inside a triangle corresponds to a polytope in \mathcal{L} having exactly four interior points which are also in \mathcal{L} . Points in the same triangle correspond to polytopes having the same four interior points, but for different triangles the polytopes have different sets of interior points. Thus each unit cell contains 26 ‘atoms,’ 22 exterior and 4 interior sites.

Each of the triangles in $\hat{\mathcal{Q}}$ is further divided into eight regions shown in Fig. 2. The points inside the quadrilateral denoted by (a1) in Fig. 2, correspond to a polytope intersecting with four other polytopes and sharing with each a polyhedron \mathcal{J} with six faces; inside the two triangles denoted by (a2) and (a3), each point corresponds to a polytope intersecting with five other polytopes and sharing with one of them a polyhedron \mathcal{K} with twelve faces and with the other four polyhedra \mathcal{J} ; inside the two other triangles (a4) and (a6), each point corresponds to a polytope intersecting with four neighboring polytopes sharing with one of them a polyhedron \mathcal{K} and with the other three polyhedra \mathcal{J} ; inside the two remaining triangles (a5) and (a7), a polytope intersects with five other polytopes, sharing with two of them a polyhedron \mathcal{K} and with the other three a polyhedron \mathcal{J} ; inside the pentagon (a8), a polytope intersects with six other polytopes sharing with two of them a polyhedron \mathcal{K} and with the other four a polyhedron \mathcal{J} . Their relative frequencies are related to the ratio of their areas and are

$1 : p^{-3} : p^{-2} : p^{-3} : \frac{1}{2}(p^{-2} + p^{-4})$. These frequencies are independent of c .

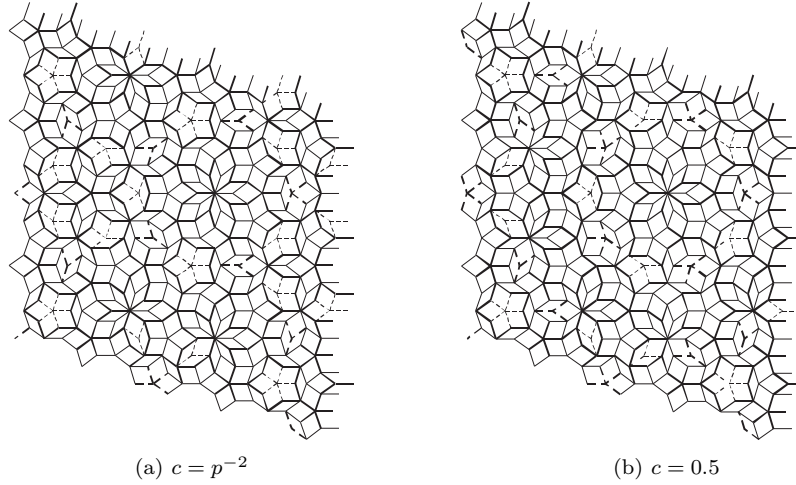


Figure 4. Generalized Penrose tilings: There are four kinds of edges. Edges connecting two sites with index 1 and index 2 are represented by a thin dashed line; edges connecting sites with index 4 and index 5 by a thick dashed line; edges connecting sites with index 2 and index 3 by a thick line; and edges connecting sites with index 3 and index 4 by a thin line. Even though no arrows are drawn on the edges, the ‘positive’ (connecting I to $I + 1$ sites) or ‘negative’ (connecting I to $I - 1$ sites) direction of an edge, is completely determined by the indices of the sites at the two ends of an edge.

The 3-d quasiperiodic lattice \mathcal{L} can be further shown to be periodic in the z -direction, which is the direction of the line joining the bottom and the top of the polytopes \mathcal{P} , and aperiodic in the xy -directions.¹⁰

6. Conclusion

The generalized Penrose tilings of thin and fat rhombs cannot be converted to tilings of kites and darts. This can be seen as follows: Four thin rhombs and one fat rhomb is the only way to fit the vertex of type $[3, 1]_2$ in Fig. 3b, which can be easily seen to be nonconvertable to a tiling of darts and kites. On the other hand, for $c = 0$, the kite-and-dart patterns of the Penrose tiling⁵ can be viewed as single repeating cartwheels,³ which overlap with their neighbors. These cartwheels are the overlapping quasi-unit-cells of Gummelt,^{5,6,7,8,9} and are larger than the decagons which are the projections of the 5-d unit cells onto 2 dimensions.¹⁷ The generalized Penrose tilings are shown to be inequivalent to kite-and-dart patterns, nor do they satisfy the

inflation and deflation rules. Therefore, the method of Gummelt cannot be used here. It can be seen from Fig. 4 that in the neighborhood of the star vertices $[5, 0]_3$ or $[0, 5]_4$, only parts of decagons which are the projections of the 5-d unit cells onto 2 dimensions¹⁷ are in \mathcal{L} . This is not like the case for $c = 0$ or for the projection of the 5-d lattice onto 3-d space. The difference may be due to the fact that 3-d cut hyperplanes in 5d are larger than 2-d cut planes and therefore contain most of neighboring unit cells $\text{Cu}(5)$. For $c = 0$, the cut plane for the Penrose tiling is special such that each decagon which is a projection of the unit cell $\text{Cu}(5)$ into \mathcal{D} can also be viewed as quasi-overlapping unit cell.

Acknowledgments

We are most thankful to Dr. M. Widom and Dr. M. Baake for providing us with many useful references and to Dr. Molin Ge, Dr. Chengming Bai and the Nankai Institute of Mathematics for their hospitality and support.

References

1. D. Shechtman, I. Blech, D. R. Gratias and J. W. Cahn, *Phys. Rev. Lett.* **53**, 1951–1953 (1984).
2. R. Penrose, in *Introduction to the Mathematics of Quasicrystals*, Aperiodicity and Order, Vol. 2, M. V. Jarić, ed., (Academic, Boston, 1989), pp. 53–79.
3. B. Grünbaum and G. C. Shephard, *Tilings and Patterns*, (W. H. Freeman and Co., New York, 1987), Ch. 10.
4. N. G. de Bruijn, *Indagationes Mathematicae* **84**, 38–52, 53–66 (1981).
5. P. Gummelt, *Geometriae Dedicata* **62**, 1–17 (1996).
6. P. J. Steinhardt and H. C. Jeong, *Nature* **382**, 433–435 (1996).
7. P. J. Steinhardt, H. C. Jeong, K. Saitoheong, M. Tanaka, E. Abe and A. P. Tsai, *Nature* **396**, 55–57 (1996).
8. P. J. Lord and S. Ranganathan, *Acta Crystallogr.* **A57**, 531–539 (2001).
9. P. J. Lord, S. Ranganathan and U. D. Kulkarni, *Philosophical Magazine* **A81**, 2645–2651 (2001).
10. H. Au-Yang and J. H. H. Perk, *J. Phys. A* in press, cond-mat/0507117.
11. N. G. de Bruijn, *Indagationes Mathematicae* **A89**, 123–152 (1986).
12. F. Gähler and J. Rhyner, *J. Phys.* **A19**, 267–277 (1986).
13. V. Elser, *Acta Crystallogr.* **A42**, 36–43 (1986).
14. M. Duneau and A. Katz, *Phys. Rev. Lett.* **54**, 2688–2691 (1985).
15. A. L. Mackay, *Physica* **A114**, 609–613 (1982).
16. M. Baake, D. Joseph, P. Kramer and M. Schlottmann, *J. Phys.* **A23**, L1037–L1041 (1990).
17. H. Au-Yang and J. H. H. Perk, *Generalized Penrose Tilings*, to be published.
18. D. Levine and P. J. Steinhardt, *Phys. Rev.* **B34**, 596–616 (1986).
19. J. E. S. Socolar and P. J. Steinhardt, *Phys. Rev.* **B34**, 617–647 (1986).